TAO, Vol. 8, No. 2, 165-178, June 1997

Ionospheric Response to a Solar Eclipse in the Equatorial Anomaly Region

K. C. Yeh[1], D. C. Yu[1], K. H. Lin[1], C. H. Liu[2], C. R. Huang[2], W. H. Tsai[2], J. Y. Liu[2], J. S. Xu[3], Kiyoshi Igarashi[4], Chufu Xu[5], W. -X. Wang[6]

(Manuscript received 31 December 1996, in final form 10 April 1997)

ABSTRACT

On October 24, 1995 a solar eclipse occurred with its path of totality passing over southern Asia, but the associated region of its partial eclipse covered almost all of Asia. It was therefore of interest to investigate how the ionosphere responded to this eclipse, especially because the region included the equatorial anomaly region. For this purpose the authors collected and processed ionosonde data from six stations in the region. These data reveal three effects that are coherent geographically in that they cover at least two of these six stations: (1) For the region with geomagnetic latitudes higher than 20 degrees, the N_{max} increased slightly immediately following the first contact for about 30 minutes. (2) In response to the eclipse, the largest depression occurring roughly 11/2 hours after the maximum obscuration was observed at approximately 14 degrees geomagnetic latitude even though the percent obscuration of the Sun at latitudes lower than 14 degrees was larger. (3) Around 6 hours after the maximum phase another secondary depression in the N_{max} was observed for geomagnetic latitudes lower than 14 degrees. Physical mechanisms that may be responsible for causing these effects are proposed and examined in this paper. They are all related to eclipse-caused dynamic effects.

(Key words: Solar eclipse, Ionospheric effects, Equatorial anomaly region, Fountain effect, Interhemispheric flow)

1. INTRODUCTION

Ionospheric phenomena occur naturally and as such, all processes usually act simulta-

[1] Department of Electrical Engineering, National Sun Yat-sen University, Kaohsuing, Taiwan 80424
[2] Institute of Space Science, National Central University, Chungli, Taiwan 32054
[3] Department of Space Physics, Wuhan University, Wuhan, Hubei 430072
[4] Communications Research Laboratory, Ministry of Posts and Telecommunications, Tokyo 184
[5] Center for Space Science and Applied Research, Academia Sinica, Beijing 100086
[6] Wuhan Institute of Physics, Academia Sinica, Wuhan, Hubei 430072

neously but with varying degrees of importance. It therefore becomes very difficult, most of the time, to sort out and isolate the causes and effects from the observed experimental data without some degree of ambiguity. The problem is compounded by the fact that the involved ionospheric processes are numerous; they include ionization, chemical reactions, ambipolar diffusion, buoyancy forces, electrodynamic drift, thermalization, neutral wind effects, etc., not to mention processes coupled into the ionosphere from the magnetosphere, the thermosphere and the lower atmosphere. A solar eclipse is one rare event by which the ionization process undergoes a predictable change somewhat rapidly, unencumbered by the slow transition of solar rays through low elevation angles, such as at sunrises or sunsets. It is for this reason ionospheric measurements during solar eclipses are of great interest.

Contained in the ionospheric literature are reports of observations of about a dozen or so previous solar eclipses. For example, early collective publications appear in Beynon and Brown (1956) and Anastassiades (1970a). More recently, Chinese scientists mounted a campaign for the September 23, 1987 solar eclipse with the results published as a book (Committee, 1990). Unfortunately, except for the abstracts, the book is written in Chinese. For non-Chinese readers, an English summary which compares the results for several eclipses can be found in He and Jiao (1993). There are also many individual publications on the results of an eclipse (e.g. Van Zandt *et al.*, 1960; Evans, 1965; Paul and Mackison, 1981; Balan *et al.*, 1982). These past measurements show that the E region ionosphere is roughly under photoequilibrium throughout an eclipse. That is, the E region ionization is mainly controlled by the changing ionizing radiation in equilibrium with the chemical processes. To a certain degree, the photoequilibrium is almost valid even in the F1 region (Van Zandt *et al.*, 1960).

The same, however, cannot be said about the F2 region where dynamic processes gain greater importance. As a matter of fact, some early F region measurements yield inconsistent results. For example, for the same eclipse event occurring on July 20, 1963, the maximum percent obscuration of the solar disc at five stations is 95 at Hamilton, Massachusetts, 95 at Westford, Massachusetts, 78 at Minneapolis, Minnesota, 73 at Danville, Illinois and 23 at Stanford, California; yet the reported maximum dip in response to the eclipse in the observed total electron content (TEC) is respectively 4×10^{16} (Klobuchar and Whitney, 1965), 2.46×10^{16} (Evans, 1965), 3.2×10^{16} (Pound *et al.*, 1966), 3.8×10^{16} (Pound *et al.*, 1966) and 2.0×10^{16} (Howard *et al.*, 1964), all in electrons/m^2. Thus, the observed dips in the TEC do not seem to show a simple and consistent relationship relative to the maximum solar obscuration. It is most likely that because of the limitations in the data, the differences in measurement methods and the manner by which the data were processed, the non-eclipse effects remain and add uncertainty to the issue. It is also possible that there exist other dynamic processes heretofore not considered. Some of these dynamic effects have very large scales (several thousand kilometers in the horizontal direction). To explain these large-scale phenomena it is necessary to assemble coordinated observational data over a large region. With the ionospheric data increasingly digitized for ease of computing, this has now, in fact, become a possibility.

This paper opens in Section 2 with a presentation and description of the ionospheric data around the October 24, 1995 solar eclipse. Further processing of the data allows for the interpretation of the results in terms of large-scale ionospheric physics. These are discussed and concluded in Section 3.

2. EXPERIMENTAL DATA

For the period October 23-25, 1995 the Sun was rather quiet with a daily sunspot number equal to 21, and a 10.7cm solar flux equal to 73×10^{-22} W/m-Hz. During this period, the magnetic activities were also low with a K_p sum of less than 15. The conditions of the October 24, 1995 solar eclipse are depicted in Figure 1. On this map, the path of totality, approximately 50 km in width, is seen skirting the southern Asian landmass into the Pacific Ocean as time progresses from 0330UT to 0500UT. Superimposed on the map are city lights showing up as black spots. Coarse latitude and longitude circles are marked every 20 degrees. Also shown are contours of the percent obscuration of the solar optical disk and the universal time at which the maximum eclipse phase occurs.

The six locations from which the ionogram data were obtained are also marked. The respective positions of the six ionosonde stations relative to the solar eclipse are important in understanding the behavior of the ionospheric response as explained later. The six stations

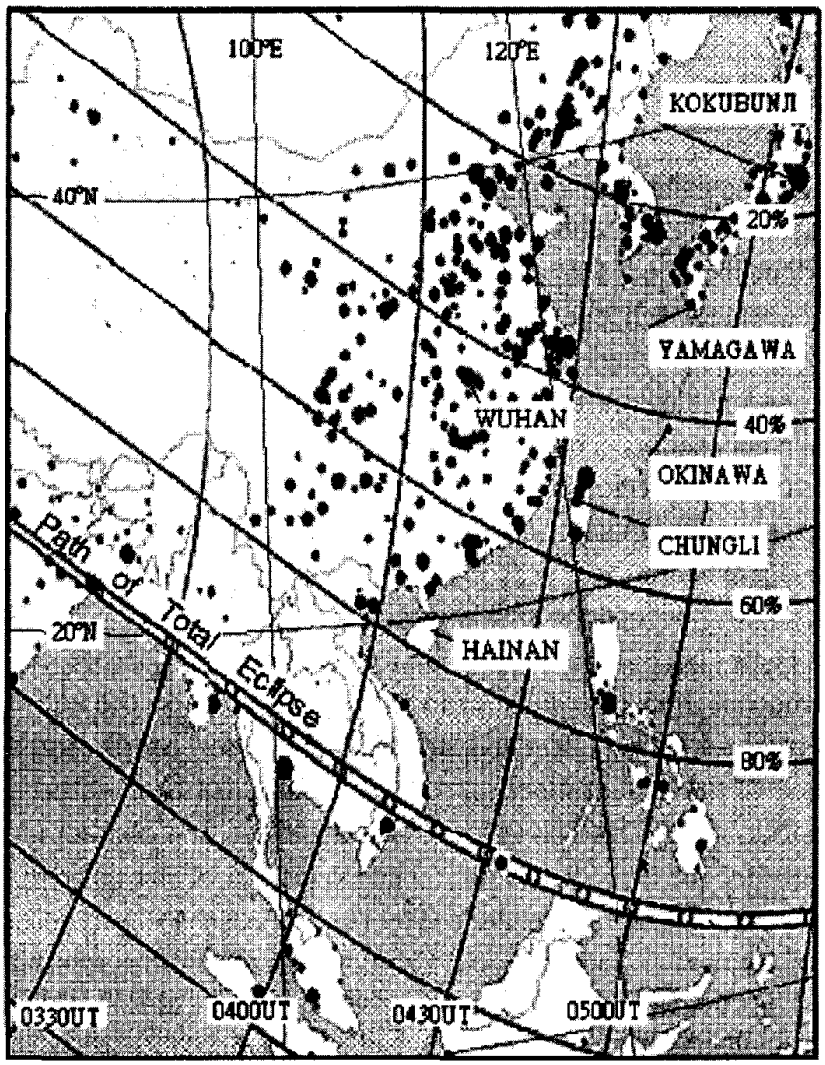

Fig. 1. Map showing the eclipse conditions and locations of six ionosonde stations. Superimposed contours depict the percent maximum obscuration of the solar optical disk and its UT time of occurrence.

have their coordinates and eclipse conditions listed in Table 1. As seen in this table, the latitudes range from 19.5°N to 35.7°N geographically but from 8.2°N to 25.4°N geomagnetically. On the other hand, the obscuration of the Sun at the maximum phase varies from 78% to 17%.

The diurnal variations of the maximum electron density N_{max} at these six stations on the eclipse day as well as one day before and one day after are plotted in Figure 2. By comparing these six plots, the equatorial anomaly behavior is easily detected for the diurnal peak on non-

Table 1. Coordinates of and the eclipse conditions at six ionosonde stations.

Station	Geographic Latitude(deg.)	Geomagnetic Latitude(deg.)	Longitude(deg.)	First Contact(UT)	Maximum Eclipse(UT)	Last Contact(UT)	Percent Obscuration
Kokubunji	35.7N	25.4N	139.5E	04:18	05:05	05:51	17
Yamagawa	31.2N	20.3N	130.6E	03:46	04:51	05:56	25
Wuhan	30.6N	19.1N	114.3E	02:53	4:10	5:29	45
Okinawa	26.3N	15.3N	127.8E	03:32	04:47	06:01	41
Chungli	25.0N	13.6N	121.2E	03:11	04:34	05:57	49
Hainan	19.5N	8.2N	109.1E	02:36	04:08	05:45	78

eclipse days. The eclipse effects also take place but do so together with some other confusing effects, the two major ones of which are the day-to-day variations and the occurrence of traveling ionospheric disturbances (TIDs). In an attempt to remove these confusing effects, several methods were applied, but eventually the two simplest ones were decided upon. In the first method, which seems to work the best, the reference day behavior is obtained by averaging the day before and the day after. The deviation of the N_{max} on the eclipse day from the reference day is then computed. The results obtained for six stations are depicted in Figure 3. It should be noted that the horizontal scale is given in hours after the first contact. The three vertical lines for each station mark the first contact, the maximum phase and the last contact, respectively. The eclipse effects are very prominent, but other non-eclipse effects still remain, especially those occurring before the first contact. As long as these side effects are minor and do not confuse the issue there is no need to be too concerned. What is of interest is to have a more accurate estimation of the depression in the N_{max} caused by the eclipse.

In the second method, in an effort to remove TID-caused oscillations, a running mean is computed at the time of the first contact on the eclipse day for each station. The reference day diurnal variation is then normalized so that at the time of the first contact its N_{max} is equal to the running mean computed for the eclipse day. The deviation of the eclipse day value from the normalized reference day is then computed. The results are displayed in Figure 4.

With the use of these two methods, the value of the maximum deviation for each station and its time delay from the maximum phase are tabulated in Table 2. For the second method, the computed normalization factors are also tabulated in Table 2. Some of the normalization factors deviate too much from unity to affect the computed electron density deviations. Nevertheless, values computed by these two methods are both included to indicate the range of possible uncertainties in the computed deviations.

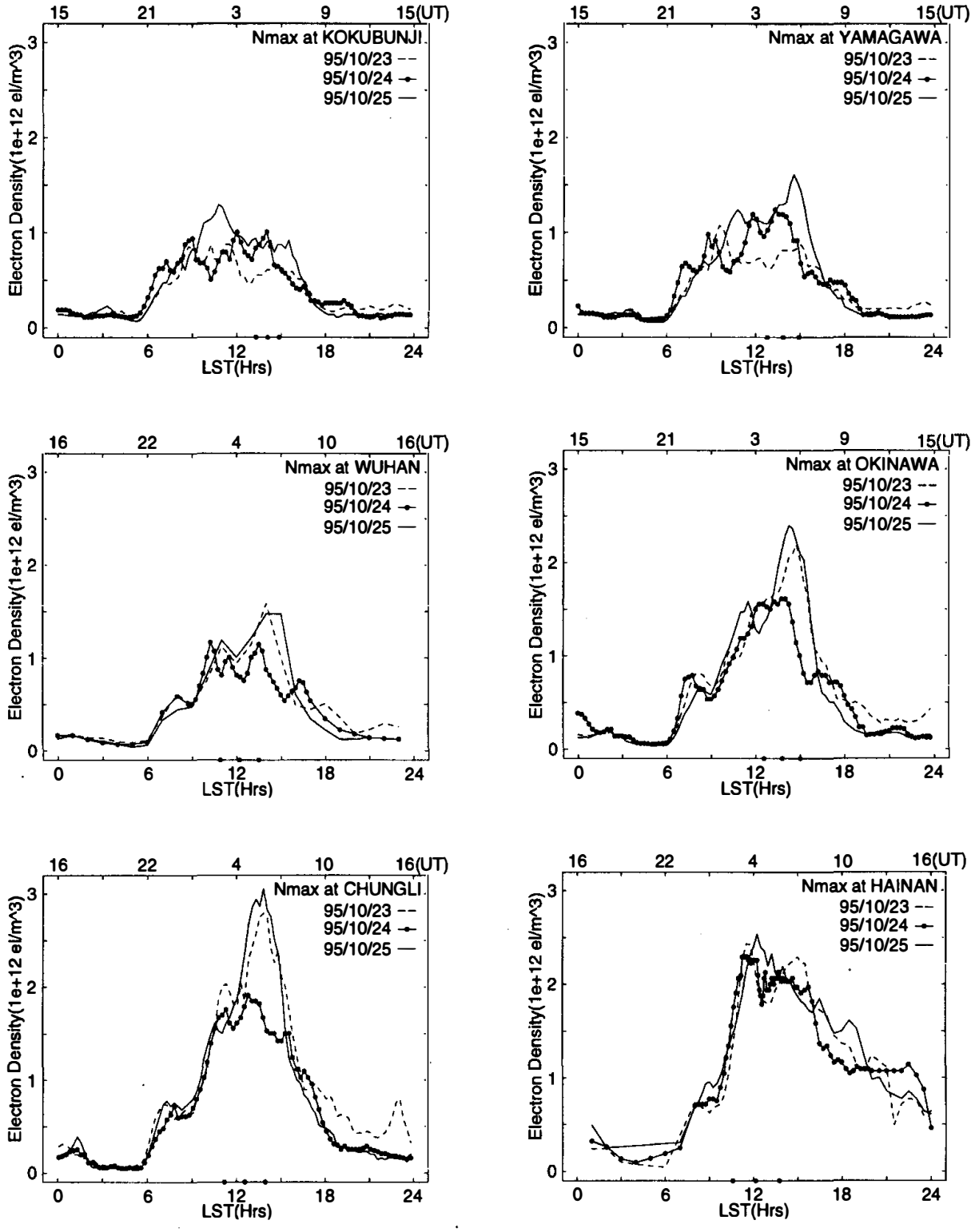

Fig. 2. Observed maximum electron density diurnal variations at the six stations on the eclipse day (October 24, 1995) as well as the day before and the day after. The local times are given at the bottom of the horizontal scale, while the universal times are given at the top. The three dots on the bottom scale mark the times of the first contact, the maximum phase and the last contact of the lunar shadow on the Sun for that station.

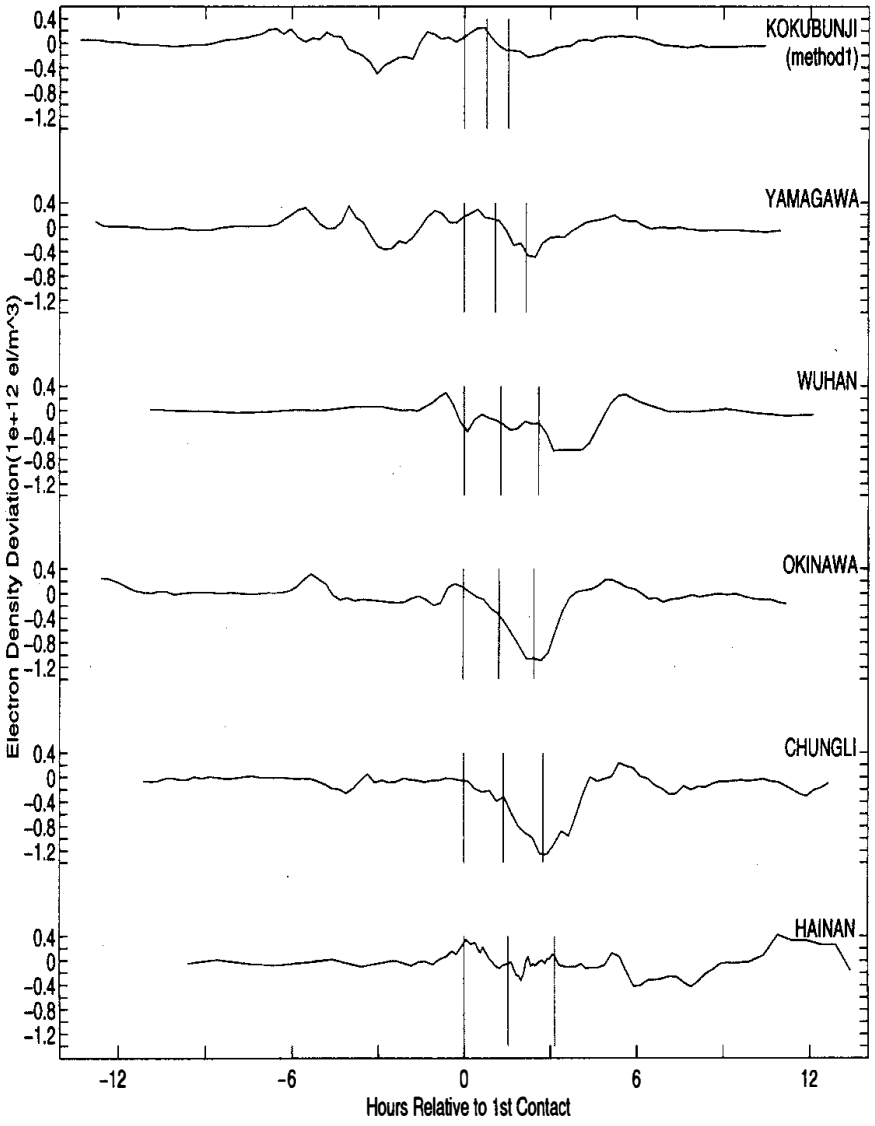

Fig. 3. Deviations in the N_{max} from the reference day at the six stations. The reference day value was obtained by averaging the values one day before the eclipse day and one day after the eclipse day. This is referred to as Method 1.

In an effort to discover the underlying physics that plays a dominant role in controlling the eclipse behavior, two plots are made. In Figure 5a, the maximum deviations as a function of percent obscuration are plotted. The vertical line is used to connect the two values computed by using these two methods. If photoequilibrium plays the dominant role in producing F2 region depressions in the electron density, the experimental points should follow a smooth curve to indicate their behavior. As seen from Figure 5a, the experimental points are somewhat scattered. In Figure 5b, the horizontal axis of Figure 5a is replaced by the geomagnetic latitude. The experimental points in Figure 5b are now better organized, especially those points using Method 1 (open circles in the Figure). It is interesting to note that the eclipse caused depression maximizes at 14° geomagnetic latitude around which the equatorial anomaly usually crests.

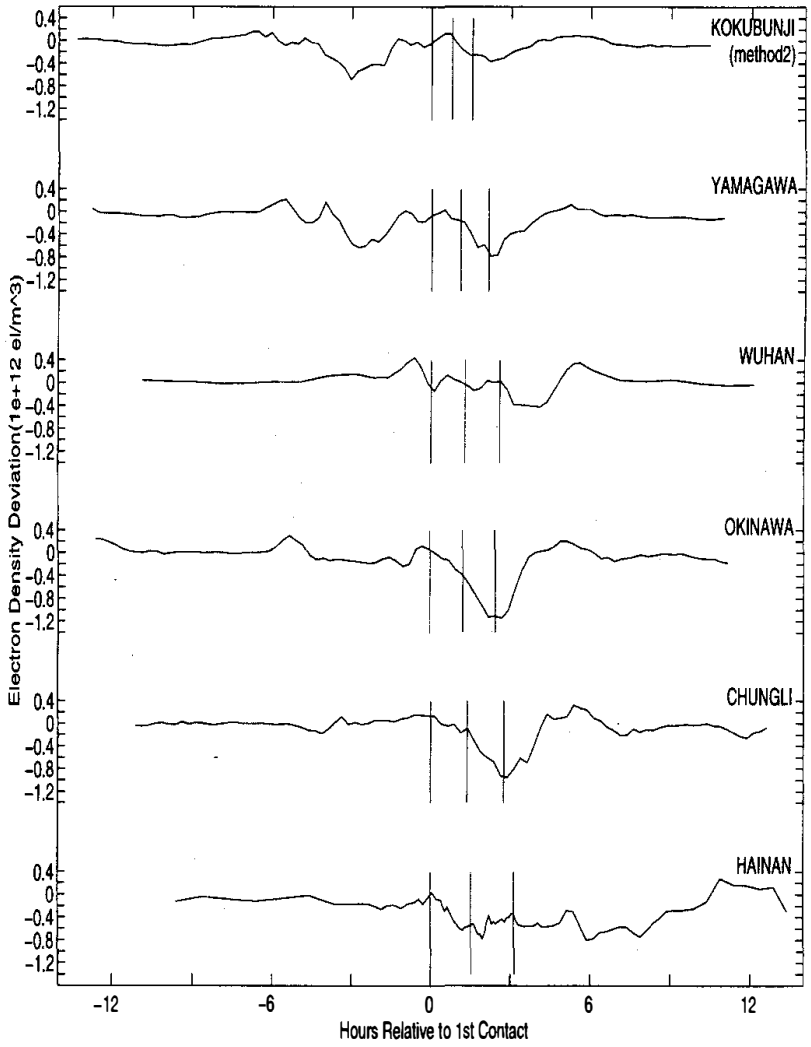

Fig. 4. Deviations in the N_{max} from the normalized reference day at the six stations. The normalized reference day value was obtained, for each station, by requiring its value at the time of the first contact equal to the running mean on the eclipse day also at the time of the first contact. This is referred to as Method 2.

Table 2. Maximum deviation in the electron density from the respective reference day values computed using two methods as explained in the text.

Station	Maximum Electron Density Deviation(Method 1) ΔN_{max} (10^{12}el/ m^3)	Time After Maximum Eclipse(Method 1)	Normalization Factor	Maximum Electron Density Deviation(Method 2) ΔN_{max} (10^{12}el/ m^3)	Time After Maximum Eclipse(Method 2)
Kokubunji	-0.229962	01:25:12	1.1796	-0.365408	01:25:12
Yamagawa	-0.486910	01:23:24	1.2732	-0.782169	01:08:24
Wuhan	-0.653722	01:49:48	0.8228	-0.417105	02:49:48
Okinawa	-1.095657	01:28:12	1.0237	-1.140916	01:28:12
Chungli	-1.263027	01:30:36	0.8890	-0.953150	01:30:36
Hainan	-0.324545	00:27:00(?)	1.2145	-0.777386	00:27:00(?)

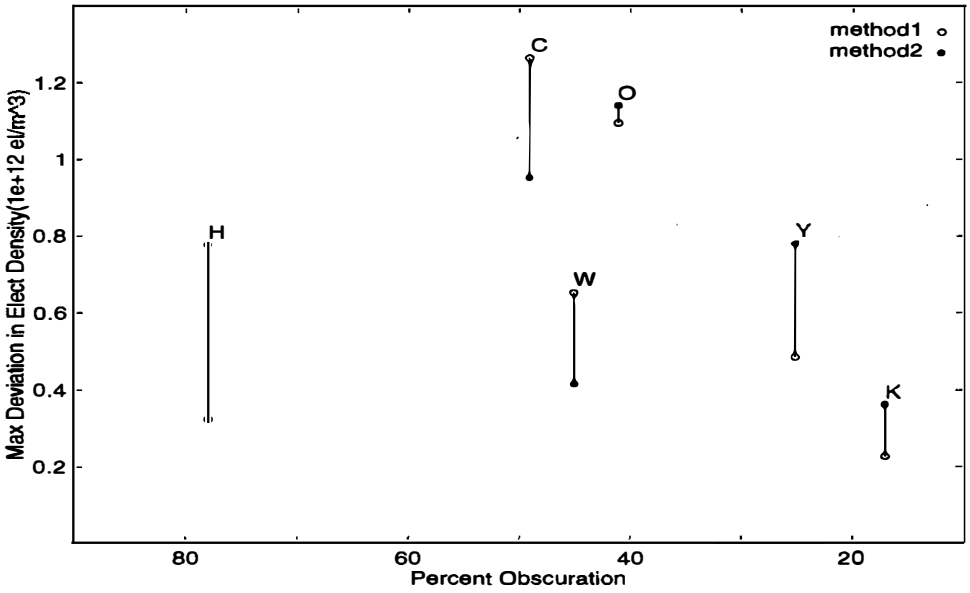

Fig. 5a. Maximum deviation in the electron density as a function of percent solar obscuration. Two methods were used to compute the reference day values.

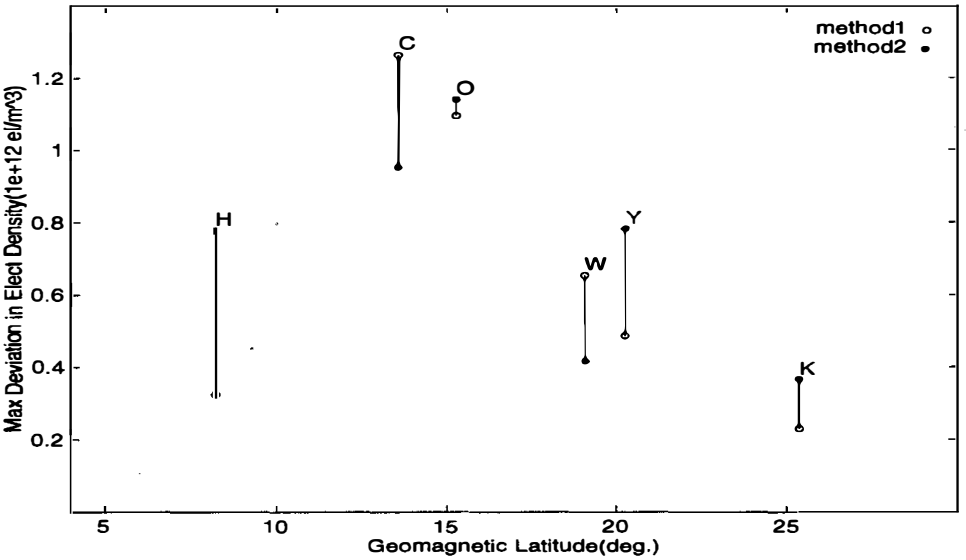

Fig. 5b. Maximum deviation in the electron density as a function of geomagnetic latitude. Two methods were used to compute the reference day values.

3. DISCUSSION AND CONCLUSIONS

During a normal day, the N_{max} as measured and reported in this paper depends on latitude, longitude and local time even when the solar conditions and atmospheric conditions are unchanged. On an eclipse day, the N_{max} is expected to be additionally dependent on the time of the first contact and percent obscuration of the Sun. Therefore, there are at least five variables on which the N_{max} can depend. Because of the geometry of this eclipse and if the data are

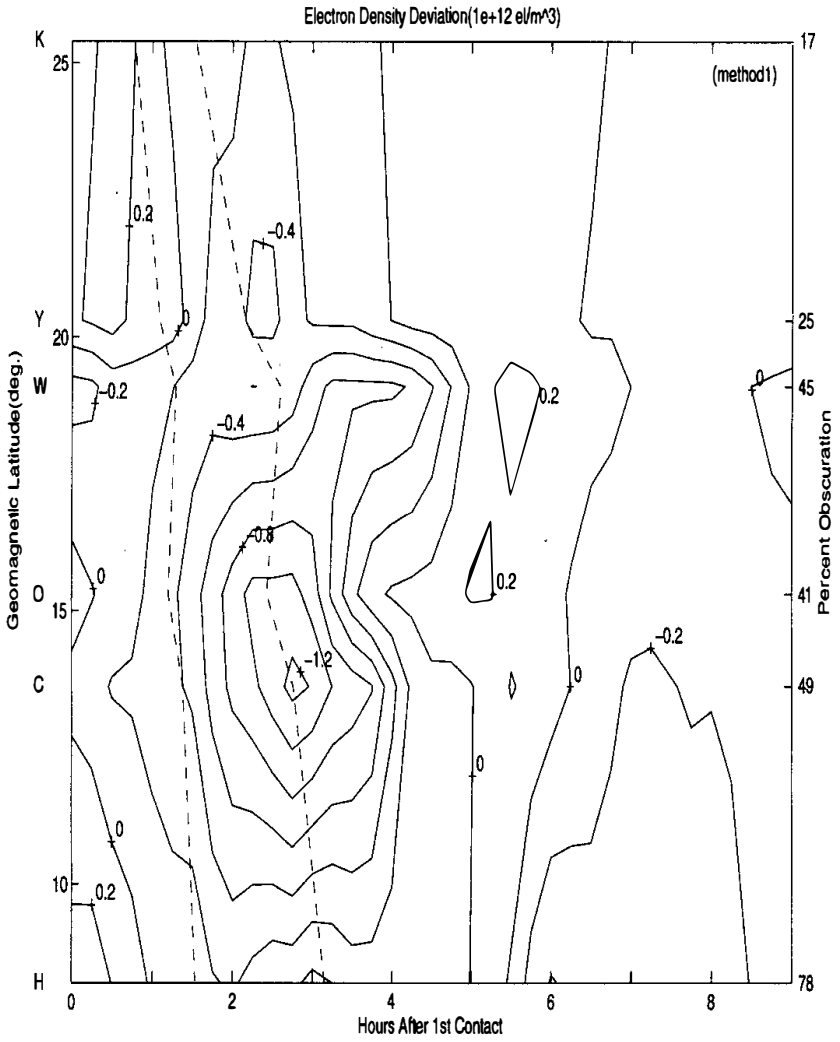

Fig. 6. Contour plot depicting the deviation in the N_{max} as a function of time (in hours after the first contact) and geomagnetic latitude. The initial letter of each of the six stations is marked on the left vertical scale, while the maximum obscuration of the solar disk for each station is indicated on the right vertical scale. The two inclined dotted vertical lines mark the time of maximum obscuration and the time of the last contact, respectively.

confined to a small longitudinal sector, some dependences may be very weak and can be suppressed. Furthermore, the results depicted in Figure 5 indicate that photoequilibrium is not a dominant force in causing the depression in the N_{max} following a solar eclipse in the equatorial anomaly region. A better organizing coordinate is the geomagnetic latitude, especially when Method 1 is used in computing the deviations. Consequently, the deviations in the N_{max} shown in Figure 3 are re-plotted as contours using the time after the first contact as the horizontal axis and the geomagnetic latitude as the vertical axis. The results are displayed in Figure 6. Along the vertical axis on the left, an initial letter of the station is used to mark each station (e.g. H for Hainan, C for Chungli, etc.). Along the vertical axis on the right, the percent of maximum obscuration of the solar disk is marked for each station. On the graph, a dotted inclined line shows the time of the maximum phase, while a second dotted inclined line shows

the time of the last contact. A careful examination of Figure 6 reveals three interesting effects that are coherent over at least two stations. (1) For magnetic latitudes higher than 20°, the initial ionospheric response is a small rise in the $N_{max.}$ which may last for about forty minutes. (2) Throughout all latitudes a major depression in the N_{max} is observed about one hour and twenty minutes after the maximum obscuration, and this major depression maximizes at about 14° geomagnetic latitude. (3) A secondary depression is observed for latitudes less than 15° geomagnetic at a time of about 6 hours after the maximum phase. In the following these results are discussed, and these three effects are interpreted in terms of ionospheric physics.

For the July 20, 1963 solar eclipse Evans (1965) used the incoherent scatter radar at Millstone Hill to observe changes in the ionospheric F region. He reported an increase in the N_{max} following the eclipse but a decrease in the electron density at 400 km altitude and higher. He attributes the increase in N_{max} as being a result of the rapid downward diffusion of ionization along the magnetic field lines, leaving an electron density deficient region above about 400 km. This downward diffusion is supported by the simultaneous observations of electron temperature to the ionic temperature ratio.

The controlling physical mechanism can be described thus. Following the first contact, the electron temperature decreases rapidly toward the ionic temperature. The reduced electron temperature leads to the downward diffusion of electrons from the topside ionosphere. Initially, the increase in the N_{max} caused by the downward diffusion may more than compensate for the decrease due to the reduction in photoionization, resulting in a small net increase. In order for this process to be effective, the electron temperature T_e must be elevated a great deal above the neutral temperature T_n, and there must also exist a large reservoir of electrons on the topside ionosphere along the magnetic field lines. Both mechanisms disfavor the geomagnetic equatorial region. Actually, Anastassiades (1970b) stated, without justification, that the magnetic dip should be at least 60° (about 40° geomagnetic latitude) for the downward diffusion process to be effective. However, recent measurements using a thermal electron energy distribution instrument on board the EXOS D satellite show a large diurnal swing in T_e above the 1000 km altitude (Balan *et al.*, 1996). At a given altitude, the daytime T_e is found to be lower at low latitudes but is still substantially higher than T_n. It is not clear if this initial small increase in the N_{max} is caused by the temperature relaxation related downward diffusion discussed above or by an entirely different mechanism. Further data are required to resolve the issue.

The second effect has to do with the major depression in the N_{max} which occurs about one hour and twenty minutes after the maximum obscuration. The fact that this major depression peaks at 14° geomagnetic latitude suggests the importance of the fountain effect. Since the 1940s (Appleton, 1946; Liang, 1947), it has been discovered that the daytime f_0F2, when plotted as a function of the geomagnetic latitude, exhibits two humps; the exact location depending on the season and perhaps with the time of day and from one day to another, but its approximate location is around $\pm 15°$ on either side of the magnetic equator. An early review of this phenomenon, known as the equatorial anomaly, can be found in Appleton (1954). Several attempts at explaining this anomaly have been made. The currently accepted theory relies on the electrodynamic drift (Hanson and Moffett, 1966). On the basis of this theory, the

$\vec{E}\times\vec{B}$ drift due to a daytime eastward electric field and the northward geomagnetic field produces an upward plasma fountain at the equator. This fountain may rise to several hundred kilometers or even to more than a thousand kilometers in altitude until the upward drifted plasma loses its momentum. Thereafter, the plasma diffuses under gravity along the geomagnetic field lines thereby forming the equatorial anomaly. The fountain and the resulting anomaly can cover a region extending to as much as 30° geomagnetic latitude on either side of the equator. Recent theoretical investigations indicate that the fountain may be influenced by the direction of neutral winds which make the anomaly hemispherically asymmetrical (Balan and Bailey, 1995). Apparently, the equatorial solar eclipse reduces the intensity of the equatorial fountain. The usual transport of ionization from the equatorial region is reduced on the eclipse day perhaps because of a weakened electrojet current flow and/or an altered neutral wind pattern. Of course, the eclipse induces a reduction in the electron density at the equator itself, resulting in a further but slight pinch in the transport.

If the weakened fountain is the correct explanation, the time required for the transport under the fountain effect from the equator is, based on the data here, about one hour and twenty minutes. At an altitude of 300 km above the 14° geomagnetic latitude, its magnetic field line rises to a 950-kilometer altitude at the equator and has a total length equal to about 2,200 km. The average velocity for the transport along the field line can then be computed to be 450 m/s which is on the high side. It should be realized that, during this time, the local photoionization effect, though weaker than the fountain effect, cannot be completely ignored. Early experimental results gave the involved photochemical time constant in the F region as approximately 30 min (Van Zandt *et al.*, 1960; Paul and Mackison, 1981). A careful examination of Figure 6 shows signs of distortions introduced by the changing photoionization effect. It should be noted that the eclipse conditions and the geometry of the path of totality in relation to the anomaly region shown in Figure 1 must play an important role in affecting this major depression. In this regard it may be interesting to keep in mind that during major magnetic storms, it is reported that electron density deviations have produced large depressions also at equatorial anomaly regions but on a global scale (Ma *et al.*, 1995). Thus, the phenomenon of equatorial anomaly is sensitive to both the major magnetic storms and the solar eclipses even though the underlining physical mechanisms may be very different.

The third effect has to do with the observed secondary depression in the N_{max} for geomagnetic latitudes of less than 14° some 6 hours after the maximum phase of the solar eclipse. In the following, two proposed causes of this effect are discussed and examined.

The Jicamarca radar data show that at the magnetic equator there exists an evening anomaly in the zonal electric field known as the post-sunset or prereversal enhancement in the vertical $\vec{E}\times\vec{B}$ drift (Fejer, 1991). This enhancement is very narrow, lasting for about one hour, and its strength varies from day to day. In the literature, three physical mechanisms have been proposed to explain this enhancement, and they have been reviewed (Eccles, 1994). Whatever the relative importance of these three mechanisms is, the electrodynamics involved must take into account the rapid decrease in the ionospheric conductivities following the solar terminator. Hence, changes in the ionospheric conductivities are the key to its cause. It is possible that the solar eclipse reduces the ionospheric conductivities and, hence, weakens the prereversal en-

hancement. If true, this may cause the N_{max} on the eclipse day to be smaller than the N_{max} during normal days around 18:00 LT. It is noted that among the six stations reported here, the two southernmost stations, Chungli and Hainan, have the largest depressions. For Chungli, the starting time of depression (i.e. reaching -0.2×10^{12} electrons/ m^3 as shown in Figure 6) is 6h40m after the first contact. This corresponds to a local time of 18:06 at Chungli, which is one hour after sunset. This starting time coincides with the usual occurrence time of the prereversal enhancement. However, for Hainan where the depression is even larger than for Chungli, the starting time (again time reaching -0.2×10^{12} electrons/ m^3) is 5h40m after the first contact. This corresponds to a Hainan local time of 15:32 which is two hours before the local sunset. The timing is, therefore, off and the previously proposed explanation as being the prereversal enhancement in the vertical $\vec{E}\times\vec{B}$ drift can be questioned for the Hainan data. To be more certain, the simultaneous vertical $\vec{E}\times\vec{B}$ drift data at the equator are required for this eclipse, but these do not seem to be available.

Another possible mechanism that may play a role in affecting the third observed effect makes use of photoelectrons coming from the conjugate ionosphere. Recent investigations indicate that there may exist substantial contributions, as much as 100% in the E and F1 regions (Titheridge, 1996) and 30% in the F2 region (Torr and Torr, 1979), to the production of ionospheric densities from secondary ionization by energetic primary photoelectrons. Apparently, in some extreme ultraviolet (EUV) radiation bands, the primary photoelectrons, after being ionized, may carry sufficient energy to produce secondary even tertiary electrons. Early studies on this photoionization problem can be found in several papers (e.g. Torr and Torr, 1979; Richards and Torr, 1988; Lilensten *et al.*, 1989). The mean free path for photoelectrons strongly depends on height, being very small in the E region and increasing rapidly with height to a value of 88 km at 300 km altitude (Titheridge, 1996). Thus, the production of secondary electrons can be considered approximately as a local process in the E and F1 regions but not higher.

In the F2 region and above, nonlocal processes, such as transport, must be taken into account. Unfortunately, numerical computations including transport are very tedious and formidable. Using steady state transport equations for photoelectron fluxes, some estimates have been made. Nagy and Banks(1970) estimated the net photoelectron escape fluxes in the 1 ev to 100 ev range to be 4.1×10^{12} electrons/m^2-sec. On an eclipse day, the conjugate ionosphere to Hainan is also under the solar shadow. Thus, a flux of 4.1×10^{12} electrons/m^2 -sec that normally arrives does not arrive on the eclipse day above Hainan. For rough calculations, the Sun is assumed to be shadowed for about one hour, resulting in a total photoelectron TEC value of 1.5×10^{16} electrons/m^2 or a contribution to the N_{max} of about 1.5×10^{11} electrons/m^3. The observed decrease on the eclipse day is 2×10^{11} electrons/m^3, which is only slightly larger than the estimated photoelectrons. Accordingly, it seems there exist enough photoelectrons to bring about an effect. Further justification would require detailed investigations, especially in view of the fact that Nagy and Banks (1970) used an excitation cross-section which was 30 times smaller than that calculated by Stauffer and McDowell (1966) and about 10 times smaller than those used by, for example, Torr and Torr (1979) and Titheridge (1996).What effect the increased excitation cross-section may have had on the escape fluxes needs to be investigated. Of interest are the questions on photoelectron flux dynamics, its secondary ionization and

thermalization processes and the question as to whether it takes 6 hours for the photoelectrons to be effective. Furthermore, a correct treatment of the problem should extend the transport equation used by Nagy and Banks (1970) to the time dependent case to take the eclipse conditions into account. This does not seem to have received attention in the literature so far.

In summary, large scale eclipse effects are observed in this study and some possible physical mechanisms causing these effects are examined. It should be noted the eclipse geometry in relation to the geomagnetic coordinates is a very important factor in producing these effects. In fact, any quantitative interpretation in terms of ionospheric physics must take this geometry into account. It is especially worth noting that in the longitude sector of the observations in this paper, the path of totality nearly coincides with the magnetic equator for the solar eclipse reported here.

Acknowledgments This research has partially been supported by grants NSC 86-2111-M-110-003-AP5 and NSC 86-2111-M-008-013-AP5 in Taiwan. The authors wish to extend their thanks to Tokuji Koizumi and Yoshihisa Masuda for scaling and supplying some of the ionosonde data.

REFERENCES

Anastassiades, M. (Ed.), 1970a: Solar Eclipses and the Ionosphere. Plenum Press, New York., 303pp.

Anastassiades, M. (Ed.), 1970b: The annular solar eclipse on May 20 1966 and the ionosphere. In Solar Eclipses and the Ionosphere, Plenum Press, 253-271.

Appleton, E. V., 1946: Two anomalies in the ionosphere. *Nature*, **157**, 691.

Appleton, E. V., 1954: The anomalous equatorial belt in the F2-layer. *J. Atmos. Terr. Phys.*, **5**, 348, 1954.

Balan, N., B. V. Krishna Murthy, C. Raghava Reddi, P. B. Rao and K. S. V. Subbarao, 1982: Ionospheric disturbances during the total solar eclipse on 16 February 1980. Proc. Indian Nat. Sci. Acad., 48A, Supplement No.3, 406-415.

Balan, N. and G. J. Bailey, 1995: Equatorial plasma fountain and its effects: Possibility of an additional layer. *J. Geophys. Res.*, **100**(A11), 21421-21432.

Balan, N., K. I. Oyama, G. J. Bailey and T. Abe, 1996: Plasmasphere electron temperature profiles and the effects of photoelectron trapping and an equatorial high-latitude heat source. *J. Geophys. Res.*, **101**(A10), 21689-21696.

Beynon, W. J. G. and G. M. Brown (Eds), 1956: Solar eclipses and the ionosphere. Pergamon Press, London.

Committee of Solar Eclipse Observations, 1990: Observations and studies in China on the annular solar eclipse of September 23, 1987. Science Publications, Beijing (in Chinese), 553pp.

Eccles, V., 1994: Examination of the equatorial electric field structure and the evening electric field anomaly. In: F.-S. Kuo (Ed.), COSPAR Colloquia Series Volume 7, pp 41-49.

Evans, J. V., 1965: An F-region eclipse, *J. Geophys. Res.*, **70**, 131-142.

Fejer, B. G., 1991: Low latitude electrodynamic plasma drifts: A review. *J. Atmos. Terr. Phys.*, **53**, 677-693.

Hanson, W. B. and R. J. Moffett, 1966: Ionization transport effects in the equatorial F region. *J. Geophys. Res.*, **71**, 5559.

He, Youwen and Peinan Jiao, 1993: The ionospheric effects of the solar eclipse. Proc. 1993 International Symposium on Radio Propagation (ISRD '93), 388-391, CIE Radio Propagation Society.

Howard, H. T., B. B. Lusignan, P. Yoh and V. R. Eshleman, 1964: Radar Doppler and Faraday polarization measurements of the cislunar medium during the July 20, 1963 solar eclipse. *J. Geophys. Res.*, **69**, 540-544.

Klobuchar, J. A. and H. E. Whitney, 1965: Ionospheric electron content measurements during a solar eclipse. *J. Geophys. Res.*, **70**, 1254-1257.

Liang, P. H., 1947: F_2 ionization and geomagnetic latitudes. *Nature*, **160**, 642.

Lilensten, J., W. Kofman, J. Wisemberg, E. S. Oran and C. R. Devore, 1989: Ionization efficiency due to primary and secondary photoelectrons: A numerical model. *Ann. Geophys.*, *7*(1), 83-90.

Ma, S. Y., L. Xu and K. C. Yeh, 1995: A study of ionospheric electron density deviations during two great storms. *J. Atmos. Terr. Phys.*, **57**(9), 1037-1043.

Maynard, L. A. and J. L. McAlpine, 1964: Total electron content measurements during the July 20, 1963 solar eclipse. *Can. J. Phys.*, **42**, 1820-1822.

Nagy, A. F. and P. M. Banks, 1970: Photoelectron fluxes in the ionosphere. *J. Geophys. Res.*, **75**, 6260-6270.

Paul, A. K. and D. L. Mackison, 1981: Scaling of the F-layer critical frequency from digital ionograms applied to observations during the solar eclipse on 26 February 1979. *J. Atmos. Terr. Phys.*, **43**(3), 221-223.

Pound, T. R., K. C. Yeh and G. W. Swenson, Jr., 1966: Ionospheric electron content during the July 20, 1963 solar eclipse. *J. Geophys. Res.*, **71**, 326-329.

Richards, P. G. and D. G. Torr, 1988: Ratios of photoelectron to EUV ionization rates for aeronomic studies. *J. Geophys. Res.*, **93**, 4060-4066.

Stauffer, A. D. and M. R. C. McDowell, 1966: An impact parameter treatment of the excitation of atoms by charged particles. Proc. Phys. Soc., 89, 289.

Titheridge, J. E., 1996: Direct allowance for the effect of photoelectrons in ionospheric modeling. *J. Geophys. Res.*, **101**, 357-369.

Torr, D. G. and M. R. Torr, 1979: Chemistry of the thermosphere and ionosphere. *J. Atmos. Terr. Phys.*, **41**, 797-839.

Van Zandt, T. E., R. B. Norton and G. H. Stonehocker, 1960: Photochemical rates in the equatorial F2 region from the 1958 eclipse. *J. Geophys. Res.*, **65**, 2003-2009.